



Volume XXII 2019

ISSUE no.2

MBNA Publishing House Constanta 2019



Scientific Bulletin of Naval Academy

SBNA PAPER • **OPEN ACCESS**

Numerical analysis of the flow around a cylinder for the perspective of correlations of the drag coefficient of the ship's hulls

To cite this article: T. Baracu and R. Boşneagu, *Scientific Bulletin of Naval Academy*, Vol. XXII 2019, pg. 256-267.

Available online at www.anmb.ro

ISSN: 2392-8956; ISSN-L: 1454-864X

doi: 10.21279/1454-864X-19-I2-031

SBNA© 2019. This work is licensed under the CC BY-NC-SA 4.0 License

Numerical analysis of the flow around a cylinder for the perspective of correlations of the drag coefficient of the ship's hulls

Tudor BARACU¹, Romeo BOȘNEAGU²

¹Ph.D.Eng, "Mircea cel Batran" Naval Academy, Constanta, Romania;
University Politehnica of Bucharest, Romania. Email: tbaracu@yahoo.co.uk

²Ph.D. Associate Professor, "Mircea cel Batran" Naval Academy, Constanta, Romania.
Email (corresponding author): romeo.bosneagu@anmb.ro

Abstract. The flow around cylinder open the path for studying more complex shape bodies like the ship's hulls. The hydrodynamic properties of the ship's hulls can be decomposed as combinations of the flow properties of simpler bodies like flat plates, cylinders, ellipses, spheres and ellipsoids. The aim of this study is to describe the flow around a cylinder based on simulations with platforms like Comsol and Ansys that further can be compared with experimental and analytical results. The drag force caused by the flow around cylinders can be combined with the drag force of simple elements like flat plates, ellipses in order to correlate with the drag force of a specific hull of ship. Cylinder is a case that offers with its simplicity the possibility to check the results in all three ways: analytical, computational and experimental. An exhaustive analysis of this shape offers a beginning path for generalizing the external flows like the application of the superposition theory for complex geometries.

Keywords: CFD, pressure drag, friction drag, external flow, drag coefficient, ship hull

1. Introduction

The external flows and their generation of drag force express a permanent challenge for design engineers activating in diverse industries (aerospace, automotive, ship building, etc). In most cases the designed shapes are very complex (walls at different angles, edges, appendices, curvature variation) and the common way is to perform CFD analysis for each given design or to use empirical formulae that use the overall dimensions of the hulls. The best way in solving those difficulties is just to relate the flow properties of the hulls with complex geometry to simpler shapes that could be better defined and solved by analytical, numerical and experimental methods.

Mainly, in this study the interest is to obtain by numerical integration the drag force distributed around cylinder for different Reynolds numbers. The interest zone is the interface cylinder – fluid where a special attention is reserved to the local meshing of the proximate flow domain considering the relative proportions of the envelope layers and a specific degree of refinement. The fluid domain was modeled with the length of ten times the diameter of cylinder in the direction of flow and five diameters on the secondary direction. The proportions chosen for the entire flow domain provide an enough distance in which the external margins of the flow area and their imposed boundary conditions do not influence distinguishable the flow near the cylinder wall.

Wieselberger (1921) came with a series of experimental results for the flow around cylinder at low and high Reynolds number and made comparisons with the Lamb's empirical formula. Roshko (1960) pointed out the closed results of the drag coefficient shared by different researches, but in the region of supercritical values of the Re number the results presented discrepancies. The applied wall interference corrections offered an increase of the accuracy of the results. Zdrakovich (1979) collected various empirical formulas for the drag coefficient recommended by several researchers especially for low Reynolds values. Spalart (1983) created a code KPD2 capable of computing the boundary layer around cylinder based on an integral method, and succeeded to eliminate some distortions in vortex

simulation that were noted in previous versions of the code. Mital (1995) did an analysis of the flow around the cylinder based on LES model of turbulence, an initiative that desired the use of an alternative method of analysis compared with the usual practices of research. He met a series of difficulties in simulation of the three-dimensional flow in the wake of the cylinder and linked them to mesh density imposed by the limitation of the available computational resources.

2. Method

For an axis-symmetrical body where a fluid flows around its surface into a direction parallel with its axis appears a pressure distribution on its surface that after summation gives an overall external load D , the drag force. It is characterized mainly by the drag coefficient C_D :

$$C_D = \frac{D}{\frac{1}{2}\rho U_\infty^2 A} \quad (1)$$

The drag coefficient is very difficult to be exactly determined analytically, because it depend on many parameters:

$$C_D = f(\text{form}, Re, Fr, \varepsilon) \quad (2)$$

At the same time, the total drag force of a body is composed by two components, friction drag D_f and the pressure drag D_p :

$$D = D_f + D_p = \int \tau \sin \theta \, dA + \int p \cos \theta \, dA \quad (3)$$

Also, the drag coefficient C_D could be put in a form of a sum between the friction drag coefficient and the pressure drag coefficient respectively:

$$C_D = C_{Df} + C_{Dp} \quad (4)$$

where

$$C_{Df} = \frac{D_f}{\frac{1}{2}\rho U_\infty^2 A} = \frac{1}{\frac{1}{2}\rho U_\infty^2} \int_0^\pi \tau \sin \theta \, d\theta \approx \frac{5.93}{\sqrt{Re}} \quad (5)$$

$$C_{Dp} = \frac{1}{A} \int C_p \cos \theta \, dA = \int_0^\pi C_p \cos \theta \, d\theta \approx 1.17 \quad (6)$$

The approximations from upper relations are as per [1]. We intend to express in later studies the drag of the specific hulls as linear combination of the drags of simpler shapes:

$$C_D = a_1 C_{D1} + a_2 C_{D12} + \dots + a_n C_{Dn} \quad (7)$$

For the flow around the cylinder, depending on Reynolds number, appear the separation of the flow from the wall of the cylinder:

- $Re < 1$ (Fig. 1): it is a creeping flow [2] where viscous forces dominates - friction drag prevail - and in this viscous flow the streamlines behind the cylinder are parallel and symmetric almost like the ones from the front of it [3] .

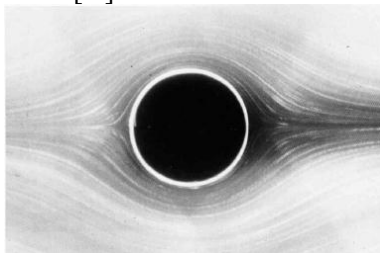


Fig. 1 The visualized flow around a cylinder for $Re=0.16$ (Van Dyke [9])

- $1 \leq Re < 30$ (Fig. 2): behind the cylinder the boundary layer begins to separate, and in the zone between the two symmetrical points of separation is appearing two twin eddies of opposed spins – Von Karman street of shed vortices; behind the two eddies the streamlines of the lateral sides of cylinder get closed together parallel and symmetric [3]. C_d depends comparable on both form drag and friction drag. C_d decreases when increasing Re .

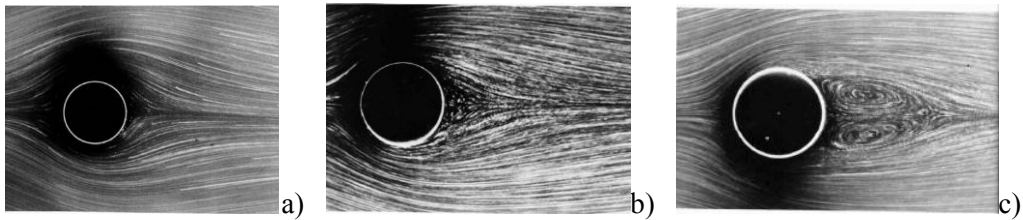


Fig. 2 The visualized flow around a cylinder a) $Re=1.54$; b) $Re=9.6$; c) $Re=26$ (Van Dyke [9])

- $30 \leq Re < 90$ (Fig. 3): periodic oscillations inside the wake of the flow behind cylinder begin to be detected [3]. C_d depends comparable on both form drag and friction drag. C_d decreases when increasing Re .

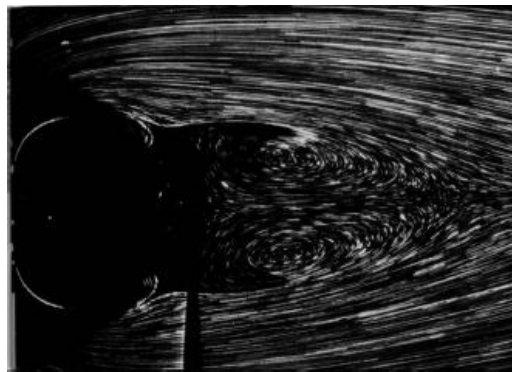


Fig. 3 The visualized flow around a cylinder for $Re=30.2$ (Van Dyke [9])

- $Re \geq 90$: the eddies alternatively spill in the backward wake of the flow and continuously regenerate on both sides of the axis parallel with the flow. C_D depends comparable on both form drag and friction drag. C_D decreases when increasing Re .
- $10^2 < Re < 10^3$ (Fig. 4): it begins the separation on a point at about 80° from the front edge. In the range of values. C_d depends comparable on both form drag and friction drag. C_D decreases when increasing Re .

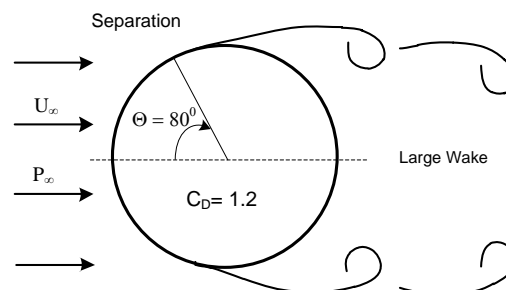


Fig.4 The flow around cylinder: the sketch of the separation point at $Re=100$, $\theta \approx 80^\circ$

- $10^3 < Re < 2 \times 10^5$ (Fig. 5a, b): it is observed that the drag coefficient is almost constant, $C_D=1 \dots 1.2$. This is because in this range pressure drag (form drag) is dominant in the total

drag. The same situation is for Strouhal number that remain almost constant around the value $S \approx 0.20$. This region practically is independent of Re number.

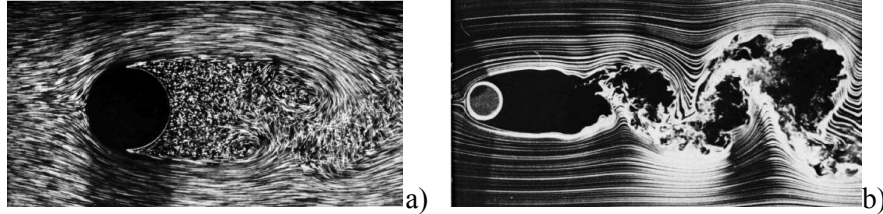


Fig. 5 The visualized flow around a cylinder: a) Re=2000, b) Re=10000 (Van Dyke [9])

- $2 \times 10^5 < Re < 5 \times 10^5$ (Fig. 6): Critical flow. At $Re = 2 \times 10^5$ the attached boundary layer begins to transit to a turbulent state because the most part of the drag is originating from the shear force that is greater for the case of turbulent flow [1] and also causes a significant drop of the drag coefficient. This effect is called **drag crisis**. It is justified by the fact that the turbulent boundary layer is more capable to resist to the adverse pressure gradient around the cylinder so it will tend to separate further back of the cylinder; the turbulent boundary layer is capable to maintain a pressure around the cylinder that reduces overall the drag. The wake will be thinner, it creates smaller vortices and determine a smaller zone of low pressure on the downstream surface, contributing to a smaller drag [2]. At $Re = 3.8 \times 10^5$ the boundary layer becomes fully turbulent and the point of separation moves further behind to around 120° from the front edge and the drag coefficient have a sudden decrease to $C_D \cong 0.3$.

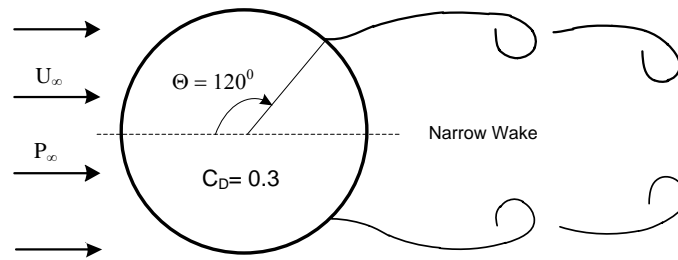


Fig. 6 Flow around cylinder: the sketch of separation point at $Re = 3.8 \times 10^5$, $\theta \approx 120^\circ$ and $C_D \approx 0.3$ = minimum

- $5 \times 10^5 < Re < 2 \times 10^6$: supercritical flow with C_D increasing slowly.
- $Re > 2 \times 10^6$: post-supercritical flow, where C_D is closed to a steady value $C_D \cong 0.67$ [4].

The most known empirical formula that describe the drag coefficient of the flow around cylinder are presented below:

- Wieselsberger-Lamb (1921) [9]: $C_D = \frac{8\pi}{Re (2.002 - \log_{10} Re)}$ (8)

- Clift (1978) [10]: $C_D = \frac{24(1 + 0.15 Re^{0.687})}{Re}$ (9)

- Munson [1]: $C_D = \frac{5.93}{\sqrt{Re}} + 1.17$ (10)

In Fig. 7 are made comparisons between the empirical formula (8), (9), (10) and the experimental values from [7].

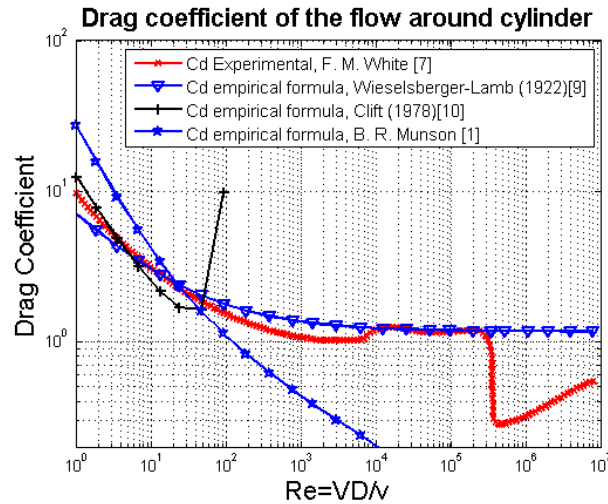


Fig. 7 – Comparison of experimental results with empirical formulas of prediction for the drag coefficient of flow around cylinder

As it is represented, neither of the presented models is capable to represent with enough accuracy the drag force for the entire range of variation of the Re number. Wieselsberger-Lamb model approximates the experiments only in a short range of the Reynolds number ($1 < Re < 10$), Clift model only in the range $1 < Re < 100$, while Munson's formula looks to cover a large range $1 < Re < 2 \times 10^5$ with good approximation (it fails in prediction of drag coefficient value only at the beginning of the drag crisis). A comparison of the mentioned empirical models (Fig. 8) recommends the one proposed by Munson model when it is desired only a reference value. The bigger share of the total drag comes from the pressure drag. Following the mathematical solutions offered by the conformal mapping studies, the pressure coefficient that governs the external flow is:

$$C_p = \frac{p - p_\infty}{\frac{1}{2} \rho U_\infty^2} = 1 - \left(\frac{U}{U_\infty} \right)^2 = 1 - \left(\frac{2U_\infty \sin \theta}{U_\infty} \right)^2 = 1 - 4 \sin^2 \theta \quad (11)$$

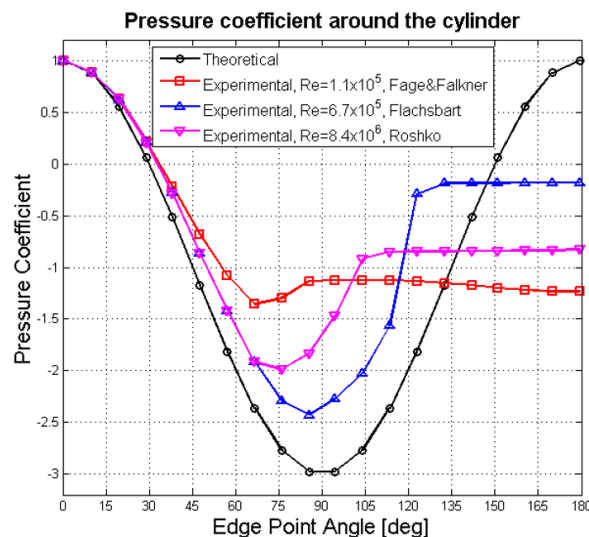


Fig. 8 Theoretical variation of the pressure coefficient around the cylinder

Strouhal number characterizes the vortex shedding in the wake of cylinder:

$$St = \frac{fD}{U_\infty} = f(Re) \quad (12)$$

The generation of vortexes and shedding encounters with a specific frequency depending on the Reynolds number. They generate fluctuations of the lift and drag coefficients that manifest as a vibration with a frequency described by Strouhal number. For $St \approx 1$ begin to dominate the viscosity in the fluid flow, and for $St < 10^{-4}$ dominates the oscillations in the wake. An empirical formula (Roshko) gives St number function of Re number ($Re < 2 \times 10^5$):

$$St = 0.212 \left(1 - \frac{21.2}{Re} \right) \quad (13)$$

The turbulence method used for analysis is $k - \varepsilon$ that is associated to the equations of Navier-Stokes in RANS form of the conservation of momentum

$$\frac{\partial u}{\partial \tau} + \rho u \nabla u = -\nabla p + \nabla[(\mu + \mu_t)(\nabla u + \nabla u')] \quad (14)$$

and equation of continuity

$$\nabla u = 0 \quad (15)$$

The $k - \varepsilon$ is the method of two equations, of turbulent kinetic energy k and of dissipation rate ε . The method iterative contains a predictor k-L (L is the turbulence eddy scale length) and a corrector ε , and the involved equations are:

- for k

$$\frac{\partial k}{\partial \tau} + \nabla \left(k u - \frac{\mu_t}{\sigma_k} \nabla k \right) = P_k - \varepsilon \quad (16)$$

- for ε

$$\frac{\partial \varepsilon}{\partial \tau} + \nabla \left(\varepsilon u - \frac{\mu_t}{\sigma_\varepsilon} \nabla \varepsilon \right) = \frac{\varepsilon}{k} (C_1 P_k - C_2 \varepsilon) \quad (17)$$

where turbulent kinetic energy k is

$$k = c_{bc} \|\vec{u}\|^2, \quad (18)$$

dissipation rate ε is

$$\varepsilon = C_\mu \frac{k^{\frac{3}{2}}}{L} \quad (19)$$

the production of turbulent kinetic energy P_k is

$$P_k = \frac{\mu_t}{2} (\nabla u + \nabla u')^2, \quad (20)$$

the turbulent viscosity of eddy μ_t is

$$\mu_t = C_\mu \rho L \sqrt{k} \quad (21)$$

the turbulence eddy scale length L is

$$L = \frac{k^{\frac{3}{2}}}{\varepsilon} \quad (22)$$

The default values of empirical parameters used in equations are

$$c_{bc} = 0.01, \quad C_\mu = 0.09, \quad C_1 = 1.44, \quad C_2 = 1.92, \quad \sigma_k = 1.00, \quad \sigma_\varepsilon = 1.30 \quad (23)$$

As initial condition, the field of velocity is considered null, then is considered a transition time τ^* of formation of a steady turbulent flow.

Near the wall the effect of viscosity prevails and while the velocity is very small, its gradient is very high and get a big amplification from closing to the wall. In order to avoid solving the equations for huge gradients of velocity, there are used wall functions that are applied at a distance y from the wall.

$$\vec{n} \cdot (\nabla u + \nabla u') = -\frac{u'^2}{\mu_t} \frac{\bar{u}}{\|\bar{u}\|}, \quad k = \frac{u_t^2}{\sqrt{c_\mu}}, \quad \varepsilon = \frac{u_f^2}{\mathcal{K} y} \quad (24), (25), (26)$$

where $\mathcal{K} = 0.42$ is the von Karman's constant. All the upper equations are applied on a surface envelope at distance y from the wall and not directly on the wall. The tangential speed u to the wall is used to calculate the frictional speed u_f :

$$\frac{\|\bar{u}\|}{u_f} = \frac{1}{\mathcal{K}} \log Re_y + \beta \quad (27)$$

Equation (27) is available in the logarithmic sublayer of the fluid near the wall and the Reynolds number has the value:

$$Re_y = \frac{u_f y}{\nu} \approx 10 \quad (28)$$

The domain is computed by using k-epsilon turbulence model that gives quality results especially near the wall where the drag coefficient can be obtained along of the boundary surface.

Flow results around a cylinder is a start in understanding the flow around more complex shapes like hydrofoils or ship's hulls where it is desired that the separation of the boundary layer to happen further back in order to assure that the flow resistance to be caused more from the viscous drag than from the pressure drag.

The domain is meshed in 2 parts (Fig. 9), such that for the near wall is used structured mesh composed of quad elements and the rest of the domain of the fluid is meshed by triangular elements. The Delaunay triangulation have specific maximization of the minimum angle inside the triangular element, avoiding skinny triangles that distorts the results. This triangulation method is commonly used in CFD for meshing the domains. On the surface of the cylinder are chosen very small elements at the scale of 10^{-4} in order to be comparable with the von Karman sublayer. Entire domain is a 16x8 m water fluid and the cylinder is 1 m diameter.

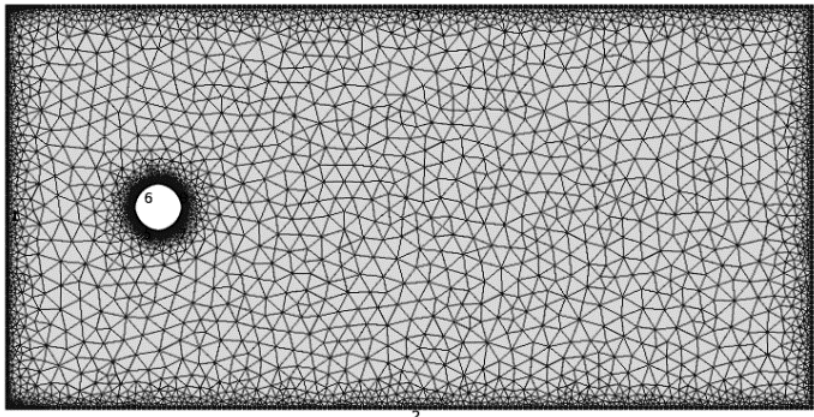


Fig.9 The mesh of the domain of flow around cylinder

3. Results

The target is the comparison of the experimental results with the numerical ones obtained by CFD analysis. Fig. 10a shows the field of velocities around the cylinder and can be distinguish that at about $30^\circ - 40^\circ$ (the angle measured from the front side of the cylinder) all the curves from the proximate zone are gathered in that point.

On the surface of the cylinder, the pressure has a maximum on front edge, then at about $30^\circ - 40^\circ$ the gradient becomes negative for any Re number. Beginning with 80° and up to 120° (the angle variation is a function of Re number) the pressure becomes null and as consequence appear the separation of the boundary layer (fig.10b).

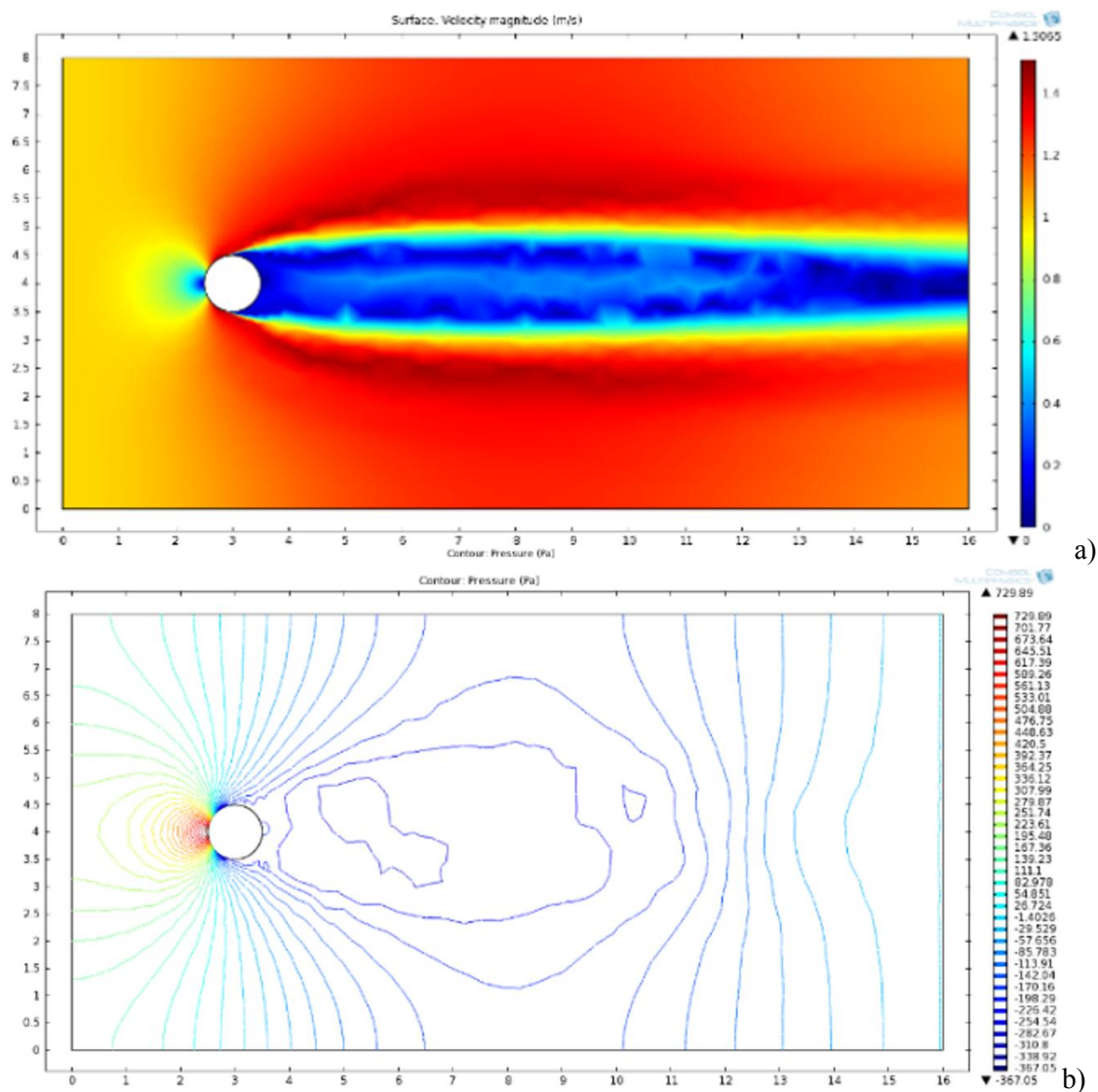


Fig. 10 Representation of the field of velocities and streamlines:
a) velocity magnitude field; b) pressure contours

Pressure coefficient describes how the external loads distribute on the surface of the cylinder. But for an overall action of the loads on cylinder is necessary to determine drag coefficient.

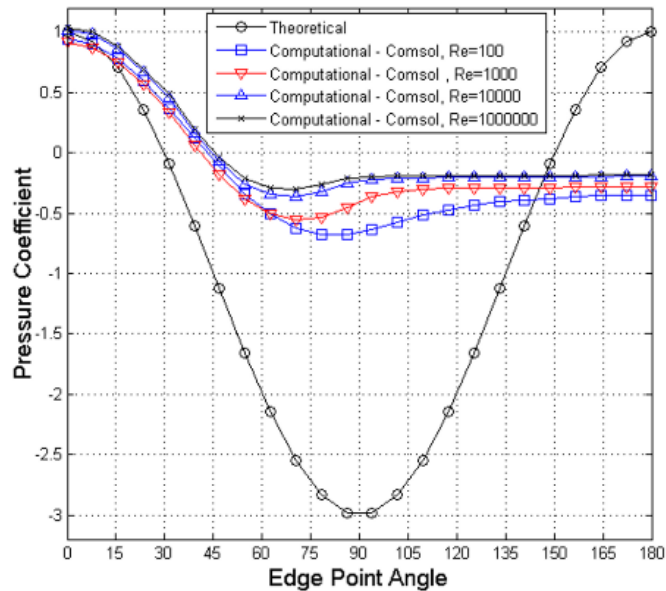


Fig. 12 Pressure coefficient of the flow around cylinder

An important issue is to try to obtain drag coefficient in a computational model and to compare it with experimental values and empirical formulas. Following this path, for a list of Reynolds numbers ($Re=10^2, 2 \times 10^2, 10^3, 2 \times 10^3, 10^4, 2 \times 10^4, 10^5, 2 \times 10^5, 10^6, 10^7$) was obtained afferent drag coefficients that gave enough information to build the drag curve.

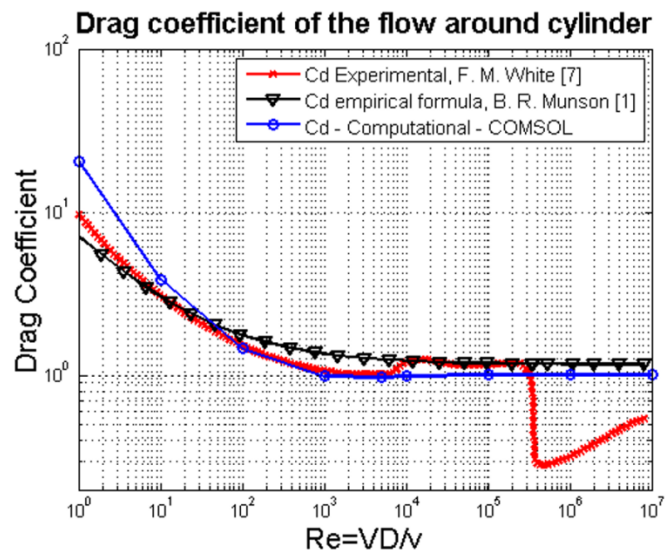


Fig. 13 Comparisons of the drag coefficient: Experimental vs Empirical formula vs Computational

The computational analysis of the model for different Re numbers got relatively closed results to the experimental values, but it is necessary to be mentioned that in the zone of the drag crisis the results differ significantly. The computational model didn't represent with accurateness the crisis zone.

The Von Karman street is also analyzed to point out the transient processes that take place in the formation and evolution of the vortices in the wake of the cylinder. Because of the transitory processes of the flow at $Re > 100$, the lift and the drag coefficients will fluctuate.

For the model of Fig. 14 are used time steps of 0.4 seconds from a total time of 320 seconds (800 time steps) for $Re=10^5$.

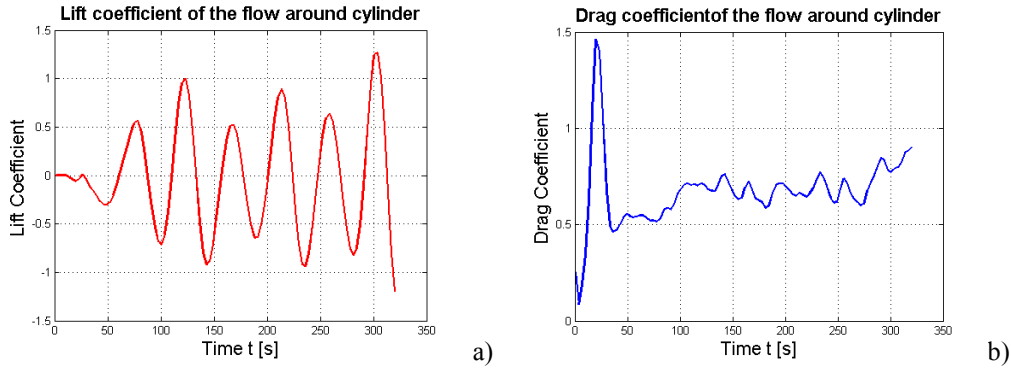


Fig. 14 Transient processes in the wake of the flow around the smooth cylinder
a) Lift coefficient; b) Drag coefficient

Analyzing the graph of the lift coefficient obtained by computation from Fig.14 a), the results show that the oscillation period is around the value $\tau = 40$ s. The lift coefficient fluctuates with the amplitude value $C_2 = 1$ while the drag coefficient with the amplitude of about $C_1 = 0.20C_L$:

$$C_D = C_1 \cdot \sin(2\pi/\tau \cdot t) \quad (29)$$

$$C_L = C_2 \cdot \sin(2\pi/\tau \cdot t) = 5C_D \quad (30)$$

The oscillation frequency is calculated in two alternative ways, by CFD analysis and similitude theory respectively:

$$f_{CFD} = \frac{1}{\tau} = 0.025 \quad (31)$$

$$f_{ST} = \frac{St U_\infty}{D} = \frac{0.2119 \cdot 0.1}{1} = 0.02119 \quad (32)$$

The relative error between the two values is:

$$Error = \left| \frac{f_{ST} - f_{CFD}}{f_{ST}} \right| \cdot 100 = 17\% \quad (33)$$

The obtained error could be reduced further if denser mesh is used but with the expense of bigger computational resources.

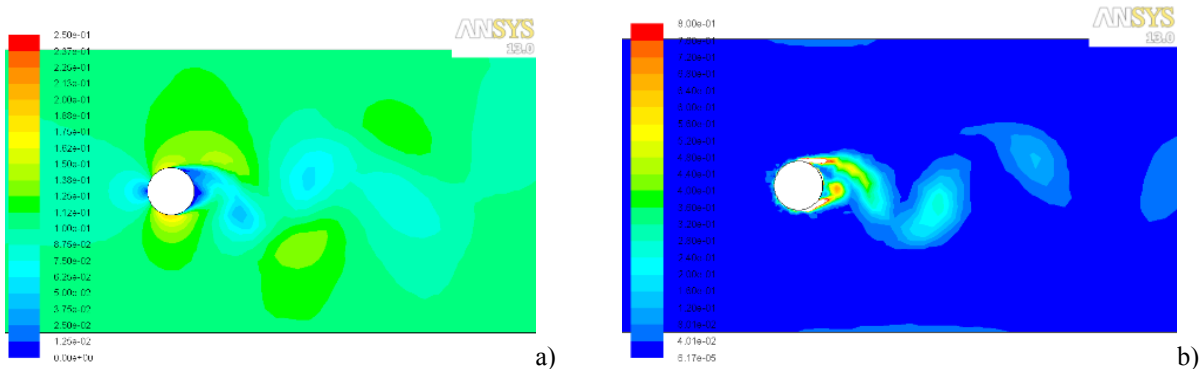


Fig. 15 Unsteady flow in the wake of the fluid flow around a cylinder:
a) Velocity magnitude; b) Vorticity magnitude

4. Conclusions

The applied computational analysis of the flow around cylinder with platforms like Comsol and Ansys shows that the CFD results keep closed to the experimental ones. In some special cases like the ones with the range of the Reynolds number localized at the crisis zone appear differences between the CFD and the experimental results. However, the CFD results for the pressure coefficient show less differences related to the experimental results.

Transient analysis for the wake of the cylinder was able to reproduce the fluid turbulence along with the creation of the two vortexes that appear at regular time steps.

The accuracy of computational analysis could be improved further by meshing with higher density the entire domain of analysis but with the expense of utilization of more powerful hardware resources.

The present results obtained the flow around a cylinder opens the path for further analysis of more complex bi-dimensional or three-dimensional shapes having at least one axis of symmetry.

The cylinder with external flow is the simplest symmetric shape where all classical methods of analysis (analytical, numerical and experimental) provide solutions making it easily processed in models of correlation of the drag coefficient of the complex shapes (like the ship's hulls) as linear combination of the drag coefficients of a list of simpler shapes.

Symbols

μ – dynamic viscosity, Ns/m²
 μ_t – turbulent viscosity, Ns/m²
 τ^* - transition time, s
 ν – kinematic viscosity, m²/s
 ρ – density, m³/s
 τ – time, s; shear stress, N/m²
 C_D – drag coefficient
 C_{Df} – drag coefficient from friction
 C_{Dp} – drag coefficient from pressure
CFD – Computational Fluid Dynamics
ST – Similitude Theory
 P_k - production of turbulent kinetic energy, N/m²/s
Fr – Froude number
k – turbulent kinetic energy, J
L – turbulence eddy scale length, m
p, p_∞ - pressure, inlet pressure, N/m²
u – speed in x direction of the model, m/s
 u_f – friction velocity, m/s
 U_∞ - inlet velocity, m/s
y – distance from the wall in boundary layer, m
A – surface of the cylinder wall, m²
Re – Reynolds number
 ε – dissipation rate
 \mathcal{K} - von Karman's constant

References

- [1] Munson B R, Young D R 2006 *Fundamental of Fluid Mechanics*, 5e., John Wiley&Sons, 2006, pp. 518-537.
- [2] Shaughnessy E J, Katz I M 2005 *Introduction to Fluid Mechanics*, Oxford Univ. Press, 2005, pp. 132-135.
- [3] Nakayama Y, Boucher R F 1999 *Introduction to Fluid Mechanics*, Butterworth Heinm., 1999, pp. 152-156.
- [4] Roshko A 1960 Experiments on the flow past a circular cylinder at very high Reynolds number, California Institute of Technology, California - USA, 1960

- [5] Crowe C T , Elger D F 2009 *Engineering Fluid Mechanics*, 9e, John Wiley&Sons. Inc, 2009.
- [6] Tropea C, Yarin A L, Foss J F 2007 *Handbook of Experimental Fluid Mechanics*, Springer, 2007, pp. 1128-1145.
- [7] White F M 1999 *Fluid Mechanics*, 4th Ed., McGraw-Hill, 1999, pp. 295 – 311, 436 – 515.
- [8] White F M 1991 *Viscous Fluid Flow*, 2nd Ed., McGraw-Hill, 1991, pp. 174 – 184.
- [9] Van Dyke, M. – *An album of fluid motion*, The Parabolic Press, Stanford, California – USA, 1988.
- [10] Wieselberg C 1922 *New data on the laws of fluid resistance*, National Advisory Comm. for Aero., 1922.
- [11] Zdravkovich M 1979 *A critical remark on use of drag coefficient at low Reynolds numbers*, Institut Mathematique, Nouvelle serie, tome 3 (11), 1979.
- [12] Mittal R 1995 *Large-eddy simulation of flow past a circular cylinder*, Center for Turbulence Research, Kanpur - India, 1995.
- [13] Hashiguchi M, Kuwahara K 1996 *Two-Dimensional Study of Flow past a Circular Cylinder*, Institute of Computational Fluid dynamics, Tokyo, 1996.
- [14] Spalart P R, Leonard A 1983 *Numerical simulation of separated flows*, NASA Technical Memorandum 84328, 1983.
- [15] Bruschi G, Nishioka T 2003 *Drag coefficient of a cylinder*, MAE171A, 2003.
- [16] Merrick R, Bitsuamlak G 2008 *Control of flow around a circular cylinder by the use of surface roughness: A computational and experimental approach*, International Hurricane Research Center, Florida - USA, 2008.
- [17] Shames I H 1995 *Mechanics of Fluids*, 3rd Edition, McGraw-Hill, 1995.
- [18] Devenport W J 2007 *Experiment 3 – Flow past circular cylinder*, AOE 3054, 2007.
- [19] ANSYS 2009 *Ansys Fluent 12.0 - Theory Guide*, ANSYS, Inc. Centerra Resource Park, 2009.
- [20] Roger W P 2011 *Multiphysics modeling using COMSOL: a first principles approach*, Jones and Bartlett Publishers, Sudbury Massachusetts, 2011.